



ISTITUTO NAZIONALE DI FISICA NUCLEARE

Sezione di Padova

---

INFN/BE-02/003

18 Ottobre 2002

HARPNote02-007

### **The HARP TOF-WALL performance and time calibration**

F. Bobisut, A. De Min, D. Gibin, A. Guglielmi, M. Laveder, A. Menegolli,  
M. Mezzetto and E. Pagan

*Dipartimento di Fisica "G.Galilei" and INFN, Padova, Italy*

M. Bonesini and A. Tonazzo

*Dipartimento di Fisica "G.Occhialini" and INFN, Milano, Italy*

#### **Abstract**

The procedure to calibrate in time the scintillation counters of the HARP TOF-WALL using cosmic muons is described in detail. The analysis of the collected cosmic events was also used to evaluate the performance of the detectors in terms of efficiency and time resolution. All scintillation counters resulted to be fully efficient. The procedure allowed to precisely align in time the signals of all counters so that an overall intrinsic time resolution of  $\sim 160$  ps could be achieved.

PACS:25.40;25.80;29.40.Mc

*Published by SIS-Pubblicazioni  
Laboratori Nazionali di Frascati*

## 1 The HARP TOF-WALL

The HARP experiment consists of a barrel spectrometer (TPC) and a forward magnetic spectrometer designed to measure charge, mass and momentum of secondary particles produced by the interaction of protons (from the PS accelerator) with targets of various elements. In the region covered by the forward magnetic spectrometer particle identification is achieved by means of Cherenkov light detection (for high momenta) and time-of-flight measurements (for low momenta). The time-of-flight is measured by the TOF-WALL, a set of 39 scintillation counters, arranged in three vertical walls (see Fig. 1), each consisting of 13 counters, positioned at about 10 meters from the target. The TOF-WALL covers an overall area of  $657 \times 243 \text{ cm}^2$ , which guarantees an almost complete geometrical coverage for the particle produced at the HARP target and deflected, according to their momentum, by passing through the spectrometer magnet.

To provide good time resolution for the highest-momentum particles ( $p > 2 \text{ GeV}/c$ ) which are expected to populate the central region, the central wall counters are shorter (180 cm) than those of the lateral walls (250 cm). The time resolution of each individual counter was measured in laboratory tests before the installation in the experimental apparatus as described in the note [1].

In each wall the counters are partially overlapped by 2.5 cm to ensure hermetic coverage. Moreover the particles which pass through the overlapping areas can contribute to cross-calibrate the counters within a given wall.

Two additional sets of scintillation counters (“calibration counters”) are placed, respectively, upstream and downstream the TOF-WALL (see Fig. 1) to trigger on cosmic events. The precise position of these counters allows the selection of cosmic muons crossing the TOF-WALL with a fixed azimuthal angle of  $\theta \sim 50^\circ$  with respect to the horizontal direction (see Fig. 2). The three downstream counters (two horizontal counters with  $L = 250 \text{ cm}$  and one vertical counter with  $L = 300 \text{ cm}$ ) provide the reference time information for the cosmic calibration procedure and are thus characterized by excellent intrinsic resolution. The upstream counters consist of two horizontal scintillators ( $L = 250 \text{ cm}$ ) and of a strip of 13 horizontal short scintillators with size  $21 \times 21 \text{ cm}^2$ . The upstream counters are removed during normal run operations with beam in order to avoid the presence of extra material in front of the TOF-WALL.

## 2 Electronics

The signal coming from each PMT is carried to an Active Splitter by high quality signal-cables (RG213). One output of the splitter, with amplitude corresponding to 100% of

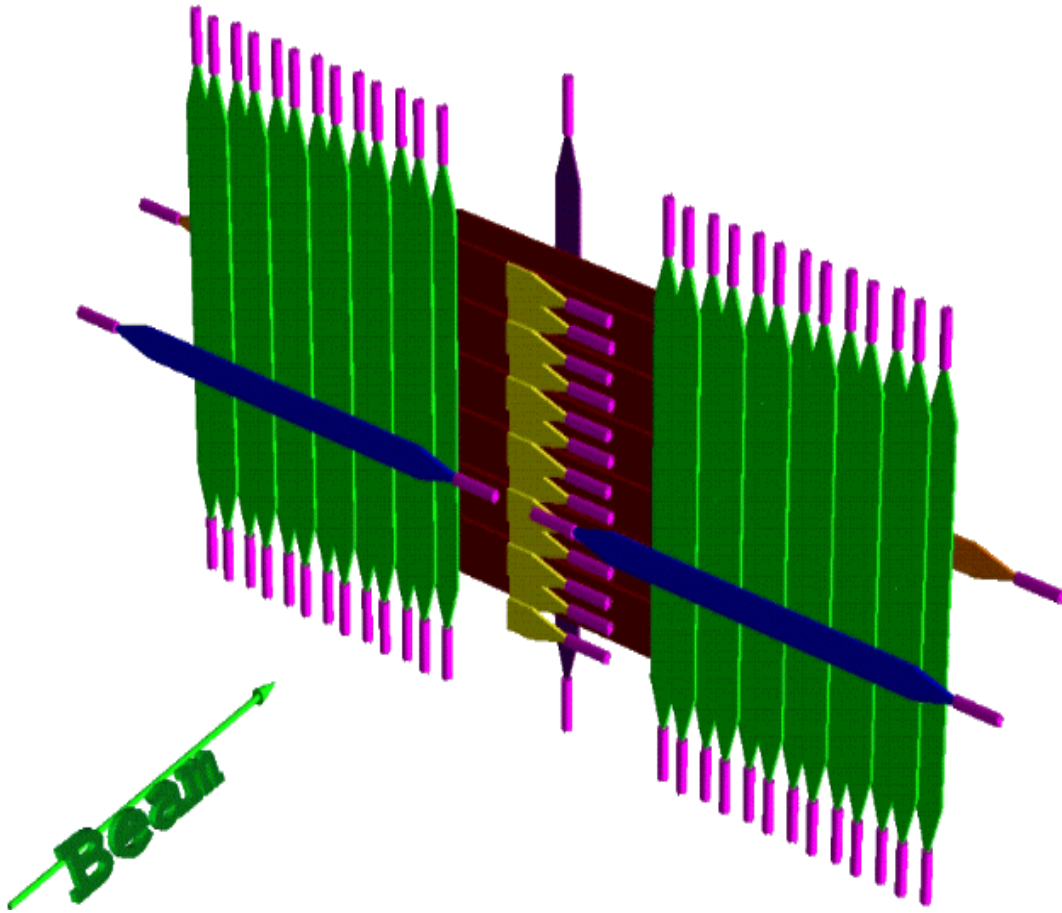


Figure 1: A sketch of the three walls composing the HARP TOF-WALL.

the input signal, is first sent to a 16-channel leading-edge discriminator (LECROY 4413) with a  $-38$  mV threshold. The discriminator signal are first delayed by  $\sim 220$  ns using a single high-quality cable, then regenerated by a fast discriminator (Line Receiver) and finally processed by the TDC's (TDC VME CAEN V775, 32 channels,  $\sim 37$  ps/ch). The second output of the splitter, corresponding to 25% of the input amplitude, is sent to a charge-integrating ADC (QDC VME CAEN 792, 12 bit,  $0.1$  pC/ch) after being delayed by  $\sim 240$  ns.

The stability of the digital electronics is monitored by pulsing simultaneously all the channels of each discriminator with an electronic signal generated by a pulser circuit. In addition the whole time-of-flight system (counters and electronics) is globally monitored through laser pulses which are directly sent to the center of each scintillator by an optical fiber injection system[2].

The trigger pulse, which defines the START signal for the TDC and the QDC gate (with  $120$  ns width), is provided by four possible sources:

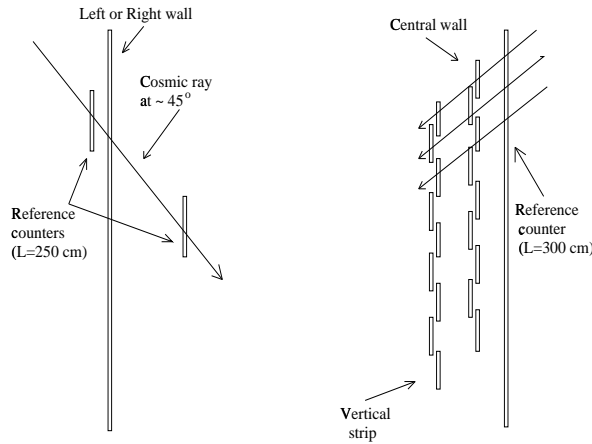


Figure 2: The centres of the TOF-WALL counters and of the cosmic trigger counters are aligned at  $\theta = 45^\circ$ ; however, if one takes into account the vertical angular distribution of cosmic muons ( $\frac{dN}{d\theta} \sim \cos^2\theta$ ) the effective average angle is  $\theta \simeq 50^\circ$ .

1. the HARP central trigger (for physics events);
2. a fast PIN photodiode (for the laser system);
3. the coincidence of signals from the cosmic calibration counters (for cosmic runs);
4. the pulser (for the monitoring of the electronics stability).

The electronics in the control room is thermostated at  $\pm 1^\circ\text{C}$ , while the counters can suffer from a maximal temperature excursion of  $\pm 4^\circ\text{C}$ , which guarantees a stability better than  $10 \div 20$  ps.

### 3 Calibration with cosmic rays

The HV settings for the PMT's were chosen on the basis of laboratory tests. The counting rate of each PMT was  $\sim 1.3$  kHz on average during the cosmic data taking, while the rate of coincidences between two PMT's attached to the same counter was approximately  $\sim 1$  kHz.

For the counter calibration about 3 million events of cosmic rays were acquired during periods of 4 days in which the beam from the PS was off; this procedure was repeated every 2-3 months during HARP data taking.

The cosmic-ray trigger was based on the signal coincidence in both the corresponding calibration counters placed upstream and downstream the TOF-wall. This resulted in an overall counting rate of  $\simeq 25$  Hz for the whole detector.

The analysis of the recorded cosmic events was used to measure the performances of the counters after the installation in HARP in terms of detection efficiencies, charge distribution and time resolution.

Each PMT resulted to be fully efficient. This was determined by comparison with its companion PMT for cosmic muons passing through the corresponding trigger counters. Moreover the study of these events allowed to determine the time offset for each PMT in order to evaluate the time-of-flight of particles inside the HARP detector.

### 3.1 The time calibration method

To properly evaluate the time-of-flight of the particles, the observed times of the PMT signals  $(t)_i^{PMT\ 0,1}$  need to be corrected in order to compensate for the time misalignment introduced by signal-cables, PMT's, discriminators, etc.. and to set the correct timing with respect to the common HARP  $t_0$  time:

$$\begin{aligned}(t^C)_i^{PMT\ 0} &= (t)_i^{PMT\ 0} + (\Delta t_-)_i + \Delta_i \\ (t^C)_i^{PMT\ 1} &= (t)_i^{PMT\ 1} - (\Delta t_-)_i + \Delta_i .\end{aligned}\tag{1}$$

In eq. (1), the term  $(\Delta t_-)_i$  corrects for the relative timing of the two PMT's for center-crossing particle and is given by:

$$(\Delta t_-)_i = \left\langle \left( \frac{t^{PMT\ 0} - t^{PMT\ 1}}{2} \right)_i \right\rangle .\tag{2}$$

The estimation of the second correction term,  $\Delta_i$ , is more involved and is obtained with a step-by-step procedure, according to the following method.

The first step consists in aligning in time the counters within each wall by correcting the times measured by the two PMT's for the time-of-flight between the  $i$ -th counter and the reference counter placed downstream the TOF-WALL:

$$TOF_i = \left\langle \left( \frac{t^{PMT\ 0} + t^{PMT\ 1}}{2} \right)_{REF} - \left( \frac{t^{PMT\ 0} + t^{PMT\ 1}}{2} \right)_i \right\rangle\tag{3}$$

by selecting the muons crossing the counters in their center with the same inclination  $\theta \simeq 50^\circ$  (see Fig. 2). The symmetry of the counter configuration allows to avoid the evaluation of  $\mu$ -path which is virtually the same for each counter with respect to the reference (the calibration counter installed behind the TOF-WALL). In the central wall this symmetry is fulfilled by requiring the coincidence of the counter of the TOF-WALL with the corresponding one in the front strip and the reference counter 300 cm long. The distance

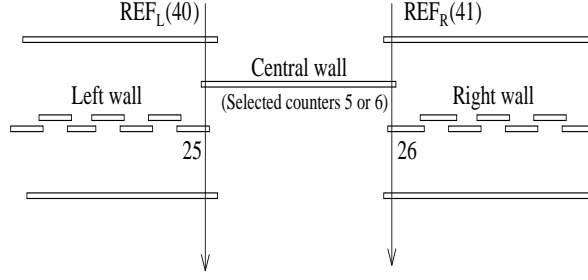


Figure 3: The setup of the the three TOF walls and of the special cosmetics counters (top view).

crossed by the muon from the reference - i.e. the calibration counter installed behind the TOF-WALL - to each counter is virtually the same for all the counters in each wall.

A second correction,  $\Delta t_1 \sim 150$  ps, takes into account the difference of flight ( $\sim 4.5$  cm) in alternate counters due to the staggering of the scintillators along the beam direction ( $\sim 2.9$  cm horizontally).

A further step consists in aligning the three walls with respect to each other using the tiny overlap regions between the central and the lateral walls <sup>1</sup> L-C-REF<sub>L</sub> and R-C-REF<sub>R</sub> (see Fig. 3):

$$\begin{aligned}\Delta t_{ref_L} &= tof(L - REF_L) - tof(C - REF_L) \\ \Delta t_{ref_R} &= tof(R - REF_R) - tof(C - REF_R).\end{aligned}\quad (4)$$

An average offset,  $\Delta t_2 \sim 670$  ps, was then introduced to take into account the shifted position along the beam direction of the lateral walls with respect to the central wall ( $\sim 12.9$  cm).

The absolute time calibration is then achieved by adding the term  $TOF_{\beta=1}$ , corresponding to the time-of-flight between the target and the TOF-WALL of particles with  $\beta = 1$ , such as high momentum non-interacting pions from the beam.

In conclusion, at the end of the correction procedure, the quantities  $\Delta_i$  are given by:

$$\Delta_i = (TOF_i + \Delta t_1) + (\Delta t_{ref_{L,R}} + \Delta t_2) + TOF_{\beta=1}.\quad (5)$$

---

<sup>1</sup>The same method can be used (with smaller statistical uncertainty) with the charged particles produced at the target in physics runs.

### 3.2 Data analysis

Among all the cosmic ray triggers, only single through-going muons traversing both the counter to be calibrated and the trigger counters, are useful for a 200 ps level calibration. Data analysis is needed to exclude spurious triggers that could spoil the final calibration. The following criteria are applied to validate useful triggers.

- Events not compatible with single through-going muons (such as *e.m.* showers or particles interacting in the detector) are rejected.
- Events crossing the edge of the trigger counters must be excluded. Their existence is shown in Fig. 4 where the distribution, as a function of the counter number, of the cosmic events recorded by the 13 vertical counters of the left wall is displayed; the trigger requires the threefold coincidence of a given scintillation counter (with both PMT's fired) with the two corresponding calibration counters (see Fig. 2). The two isolated peaks at the right side of the plot refer to the two trigger counters. The small background at the left side of the plot refers to events crossing the edge of the trigger counters and passing through the central wall in the  $\sim 6$  cm overlap region.

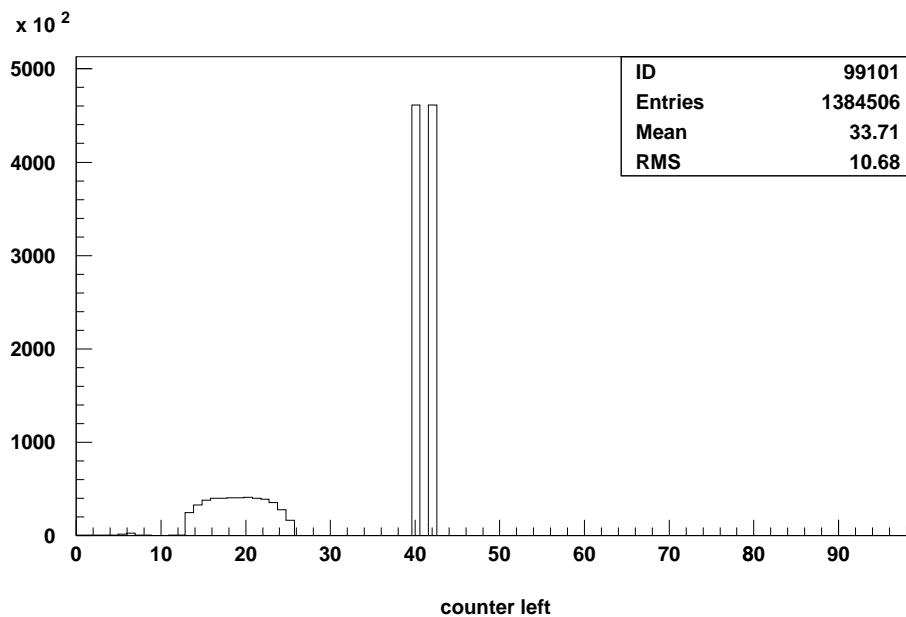


Figure 4: Event distribution for left wall counters and for the relative trigger counters (40 and 42). The counter numbering is: 0 - 12 = central wall counters; 13 - 25 = left wall counters; 26 - 38 = right wall counters.

The study of the charge spectra (pedestal subtracted) recorded by single PMT's in the data sample passing the previous selection shows the presence of events with very low signals in both PMT's of the reference counter, in correspondence with a large signal in both PMT's of the TOF-WALL counter (see Fig. 5). These events, which hit the edge of the trigger counters, would require large time-walk corrections (see Sec. 3.3); they are easily removed by the request  $Q_{REF}^{PMT\ 0, PMT\ 1} > 500$  QDC counts (left wall),  $Q_{REF}^{PMT\ 0, PMT\ 1} > 400$  QDC counts (right wall) and  $Q_{REF}^{PMT\ 0} > 200$  QDC counts and  $Q_{REF}^{PMT\ 1} > 350$  QDC counts (central wall).

- Double hits in the same counter alter its timing response. They can be produced by electromagnetic showers or gamma conversions. The distribution of the time difference  $\Delta t_-$  between the two PMT's of a few selected counters is shown in Fig. 6: the resolution  $\sigma_{\Delta t_-}$ , which includes the contribution due to the transverse size of the calibration counters ( $\sim 21$  cm), is  $\sim 340$  ps. These distributions show tails which extend well beyond the maximum time difference of  $\sim 1$  ns (with respect to the mean) expected from the transverse size of the calibration counter. Since these events are typically produced by *e.m.* showers and  $\gamma$  conversions, triggers with  $|\Delta t_-| > 1$  ns from the mean value of each counter were discarded.
- After applying the correction for the time difference  $(\Delta t_-)_i$ , see eq. (2), the events relative to each counter were selected by requiring that the longitudinal position of the particle in the reference counter, as reconstructed with the  $\Delta t_-$  information through the relation

$$\Delta t_- = \frac{t^{PMT\ 0} - t^{PMT\ 1}}{2} = \frac{x}{v_{eff}} \quad (6)$$

$$v_{eff}^{-1} \sim 6.4 \text{ ns/m}, \quad (7)$$

was corresponding to the examined TOF-WALL counter. In fact the events were selected by imposing a time-window  $\Delta t_- \sim 1.34$  ns on the reference counter, centered on the 21 cm region facing the corresponding TOF-WALL counter (see eq. (6) and eq. (7)). This value of  $\Delta t_-$  agrees with the total width of the  $\Delta t_-$  distribution for the reference counter (see Fig. 7), which covers the range  $-7.8 \div 7.8$  ns ( $1.34 \text{ ns} \times 13 \text{ counters} \simeq 15.5 \text{ ns}$ , once excluded the 2.5 cm of the overlap regions of the counters). The events recorded on the central wall were selected by requiring the coincidence of a TOF-WALL counter with the corresponding trigger counter at  $\theta = 45^\circ$  in the vertical strip.



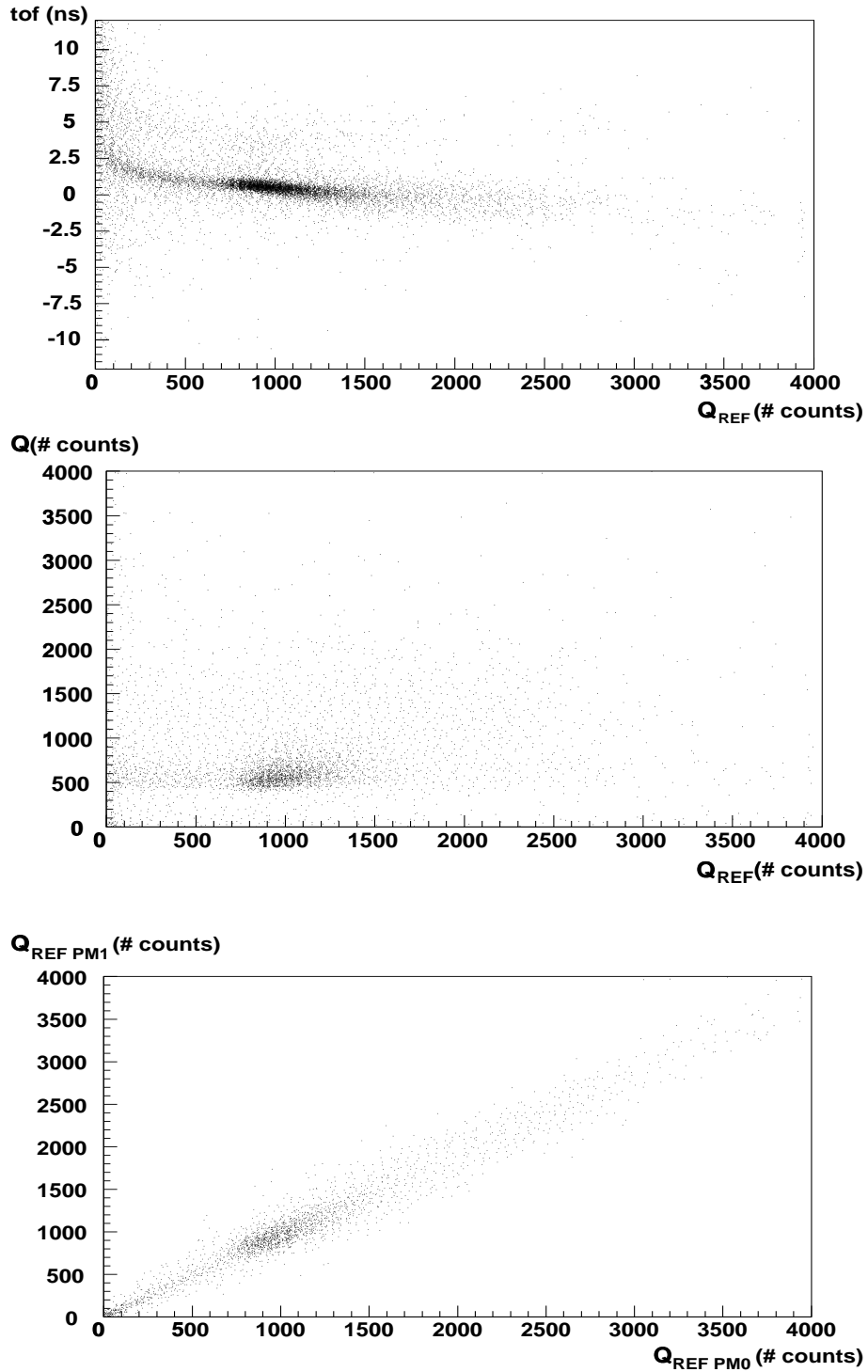


Figure 5: Above: TOF between the left wall calibration counter and counter 18 in the left wall as a function of the charge  $Q_{REF_L}$  collected by one of the two PMT's in the calibration counter. Center: charge collected by one of the two PMT's of counter 18 as a function of  $Q_{REF_L}$ . Below: charge collected by the Right PMT of the left wall calibration counter as a function of the charge collected by the Left PMT of the same counter.

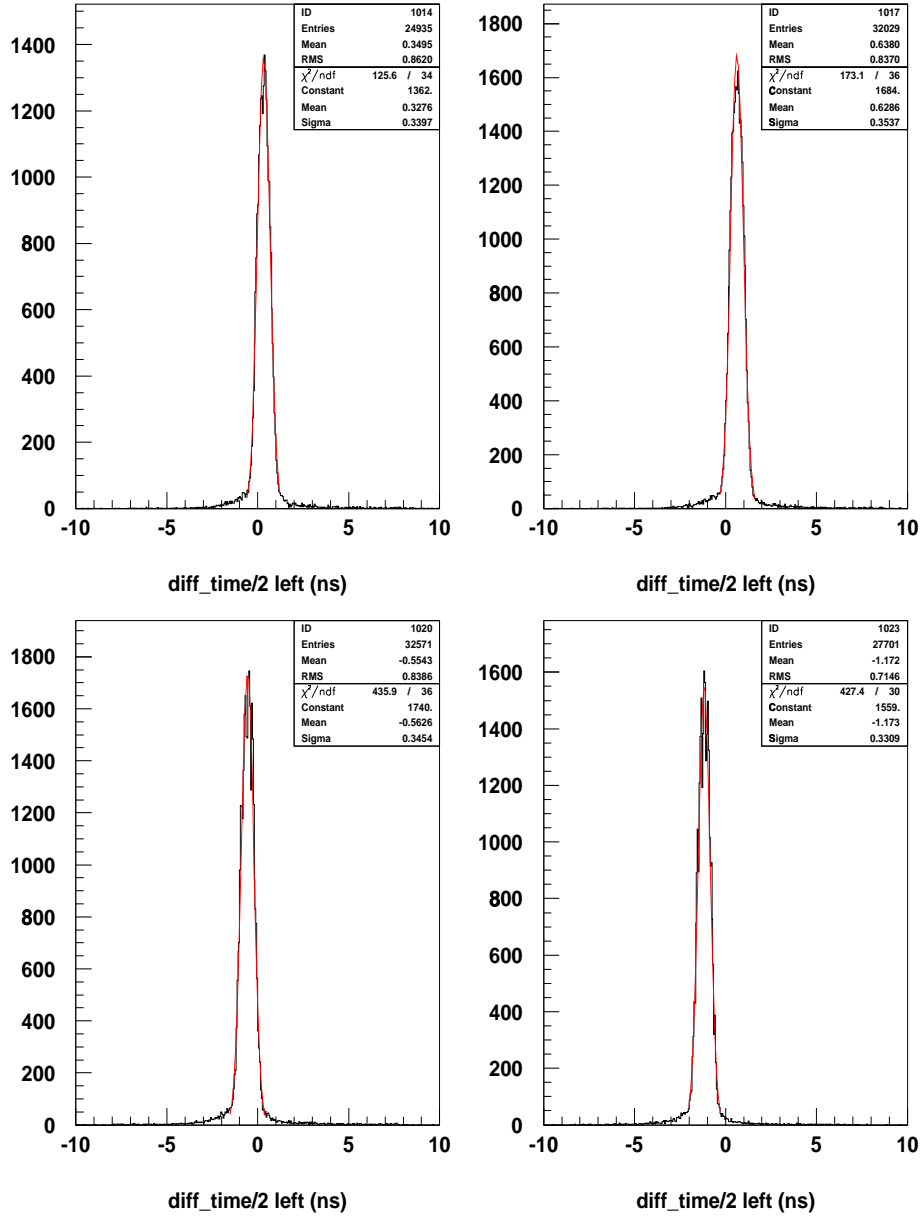


Figure 6:  $\Delta t_-$  distribution for counters 14, 17, 20 and 23 of the left wall.

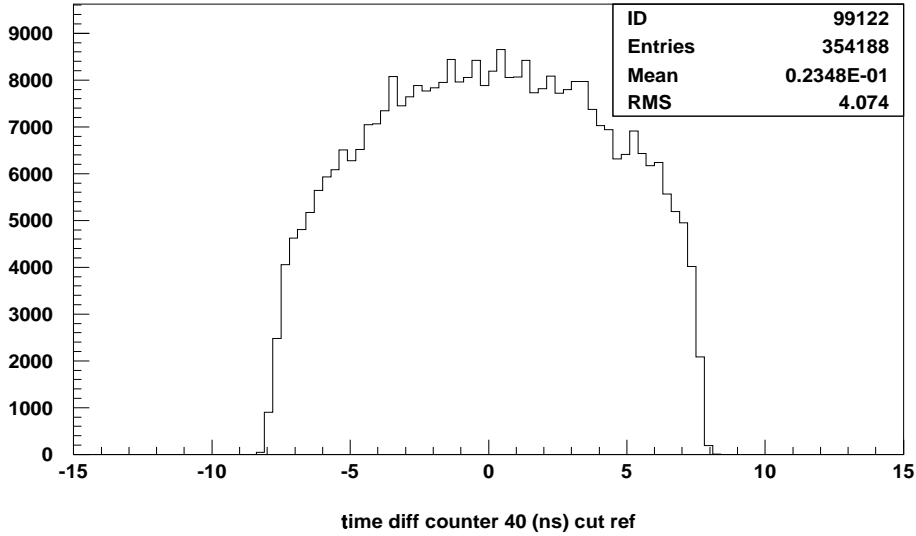


Figure 7:  $\Delta t_-$  distribution for the left wall reference counter.

- Fig. 8 shows some charge distributions of the selected events for some counters of the left wall: the spurious events producing the peak around  $Q \sim 50$  QDC counts were eliminated by requiring the charge to exceed 125 QDC counts.

### 3.3 Results

The raw times-of-flight measured between the TOF-WALL counters and the corresponding references,  $TOF_i = \langle (\frac{t^{PMT\ 0} + t^{PMT\ 1}}{2})_{REF} - (\frac{t^{PMT\ 0} + t^{PMT\ 1}}{2})_i \rangle$ , have a symmetric distribution which, as expected, is not centered around a single value of reference (see Fig. 9). The resolution  $\sigma_{TOF}$  on the time-of-flight measurement, as evaluated through a Gaussian fit, resulted to be  $\sim 280$  ps, corresponding to an intrinsic time resolution  $\sigma_I$  of 200 ps.

The distribution of the  $TOF_i = \langle (\frac{t^{PMT\ 0} + t^{PMT\ 1}}{2})_{REF} - (\frac{t^{PMT\ 0} + t^{PMT\ 1}}{2})_i \rangle$  as a function of the corresponding integrated charges  $Q_i$  shows a moderate dependence of the t.o.f. on the charge (see Fig. 10). Such a time-walk dependence can be expressed by the characteristic function

$$\delta t = W \left( \frac{1}{\sqrt{Q_0}} - \frac{1}{\sqrt{Q}} \right),$$

where  $Q$  is the event charge,  $Q_0$  is the peak of the charge distribution and  $W = 11.4 \text{ ns} \cdot \text{pC}^{1/2}$  for all PMT's.

This time-walk correction improves the time-of-flight resolution by  $\sim 60$  ps on average (see Fig. 11).

The overall distributions of the time-of-flight for the three walls are shown in Fig. 12,

13, 14, respectively. The distributions obtained after the  $TOF_i$  alignment corrections - first step in the procedure of Sec. 3.1 - confirm the effective alignment of the times in the walls and provide an estimate of the resolutions  $\sigma_{TOF} = 224$  ps (left wall),  $\sigma_{TOF} = 233$  ps (right wall) and  $\sigma_{TOF} = 222$  ps (central wall).<sup>2</sup>

The three walls were then aligned in time by comparing the times-of-flight as described in eq. (5). For this purpose the following time-of-flight distributions were reconstructed for the left wall (calibration counter 40) and the right wall (calibration counter 41), respectively (see also Fig. 3), once corrected the time-of-flight difference between counters 5 and 6 of the central wall due to the staggering of the scintillators along the beam direction (150 ps, see 3.1):

tof(40-25) with the selection of counter 5 (central wall).  
 tof(40-25) with the selection of counter 6 (central wall).  
 tof(40-5) with the selection of counter 25 (left wall).  
 tof(40-6) with the selection of counter 25 (left wall).

tof(41-26) with the selection of counter 5 (central wall).  
 tof(41-26) with the selection of counter 6 (central wall).  
 tof(41-5) with the selection of counter 26 (right wall).  
 tof(41-6) with the selection of counter 26 (right wall).

The overall distributions, obtained by summing up the events  $tof(40 - 25)$  and the events  $tof(40 - 5)$  and  $tof(40 - 6)$  (same for the right wall), are shown in Fig. 15. The peak values were used to calculate the differences  $\Delta t_{ref_{L,R}}$  between the times-of-flight as expressed by eq. (5), obtaining:

$$\begin{aligned}\Delta t_{ref_L} &= tof(L - REF_L) - tof(C - REF_L) = 0.638 \text{ ns} \\ \Delta t_{ref_R} &= tof(R - REF_R) - tof(C - REF_R) = 4.598 \text{ ns}.\end{aligned}\tag{8}$$

Using these values and the fixed correction described in Sec. 3.1, all the counters belonging to the three walls could be properly aligned in time.

The precision on the time calibration constants was estimated to be  $\sim 50$  ps, essentially dominated by the difference in angular acceptance introduced by the c-rays trigger for the counters at the edges of the left and right wall with respect to the counter at the center.

---

<sup>2</sup>The quoted values are the estimate of the resolution of the time-of-flight between the counters of the TOF-WALL and the reference ones.

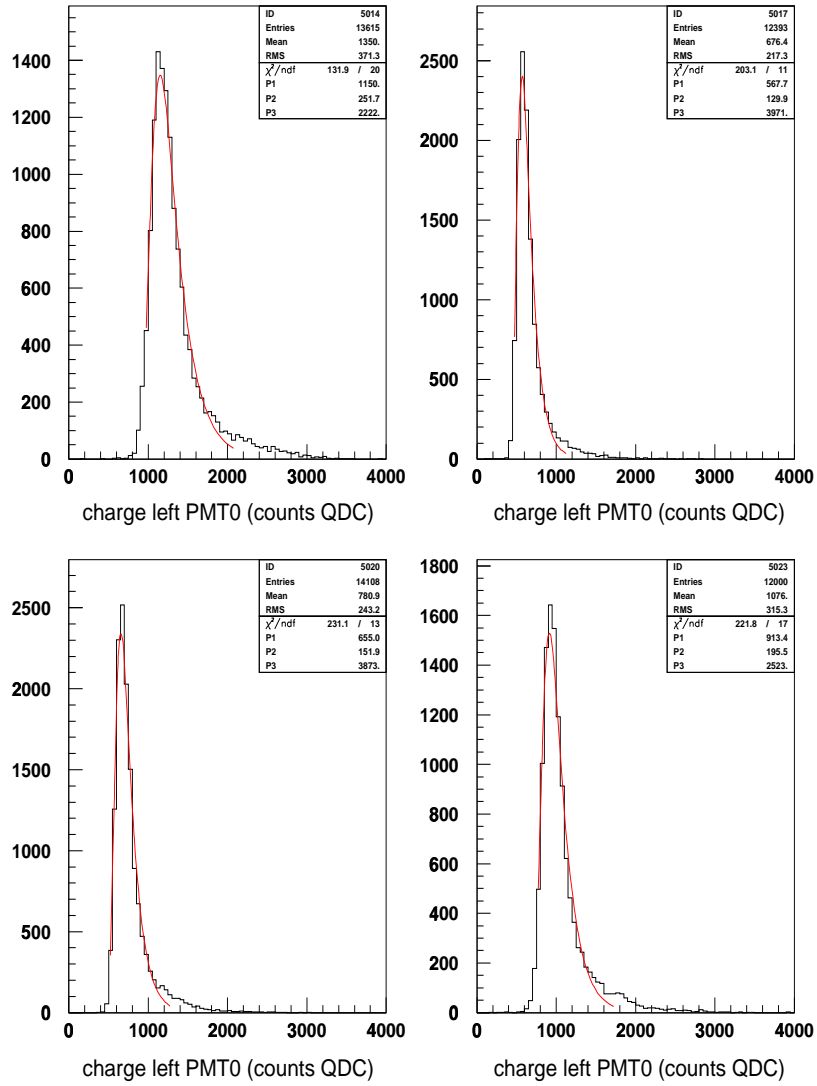


Figure 8: Charge distribution for the Left PMT's of some left wall counters (14, 17, 20 and 23).

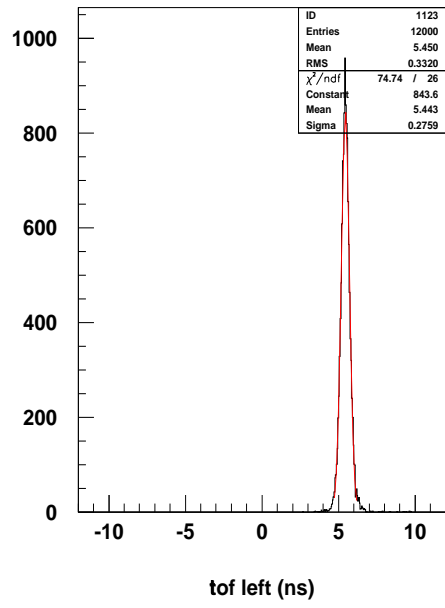
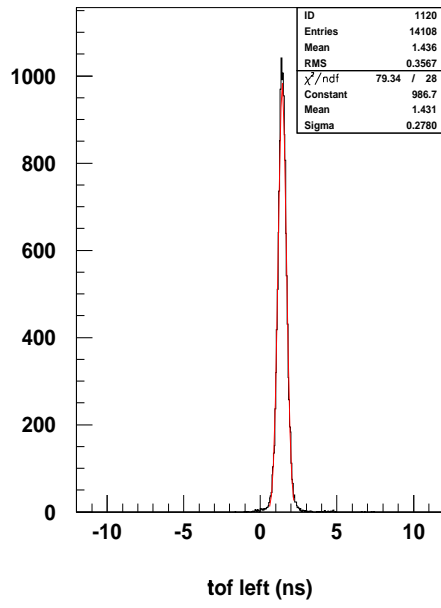
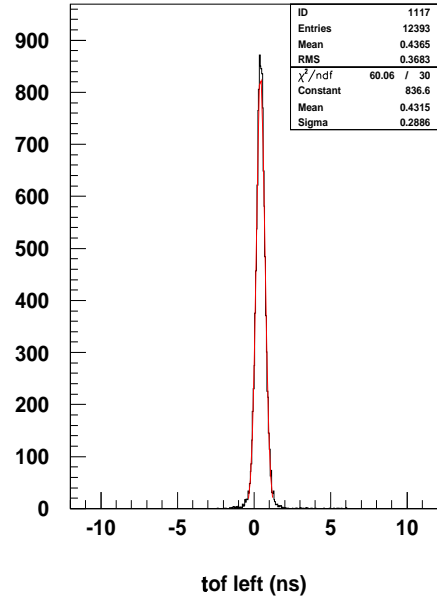
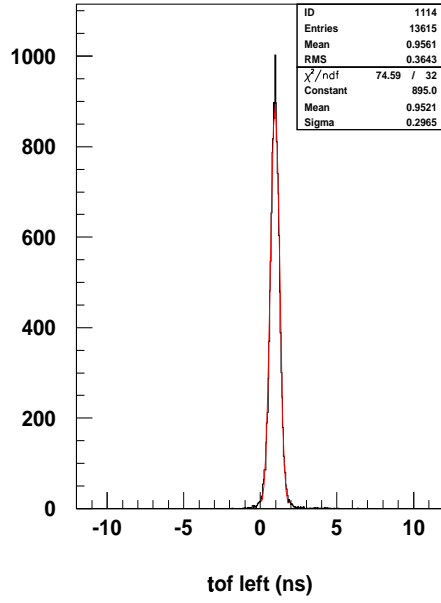


Figure 9:  $TOF_i$  distribution for  $i = 14, 17, 20$  and  $23$  (left wall).

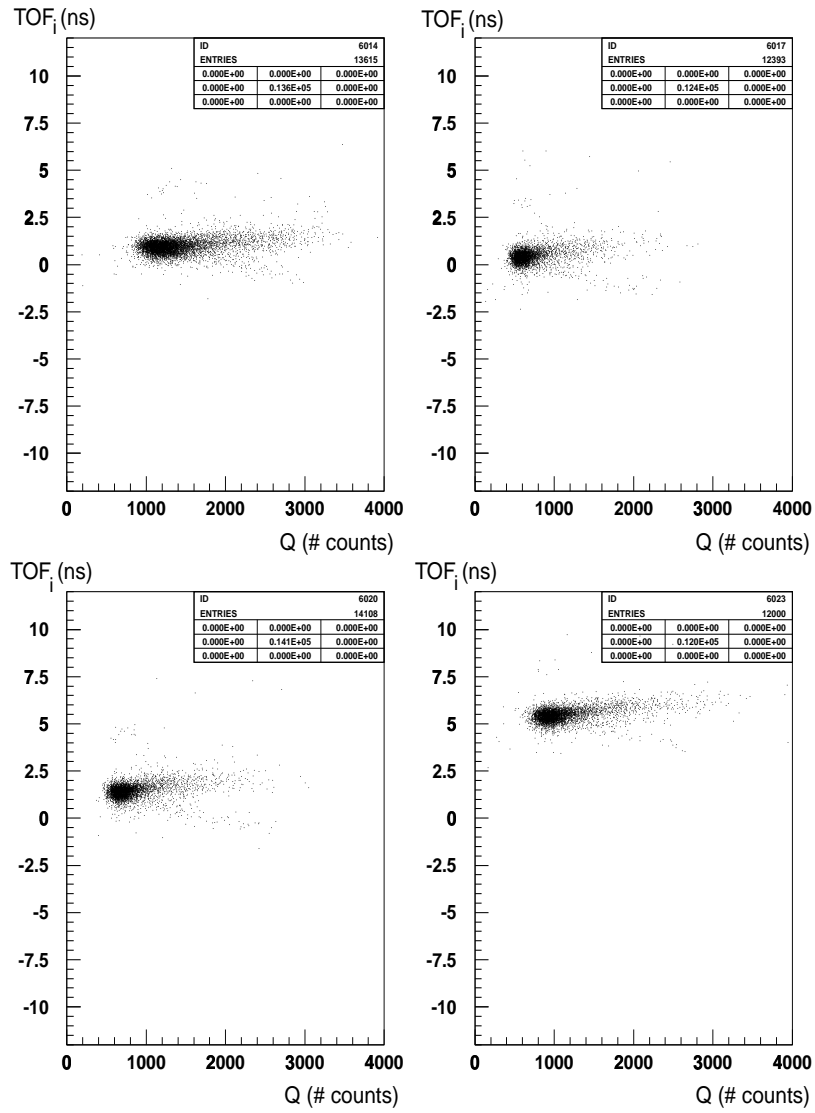


Figure 10: Dependence of  $TOF_i$  from the charge  $Q$  for PMT 0 and  $i = 14, 17, 20$  and  $23$  (left wall).

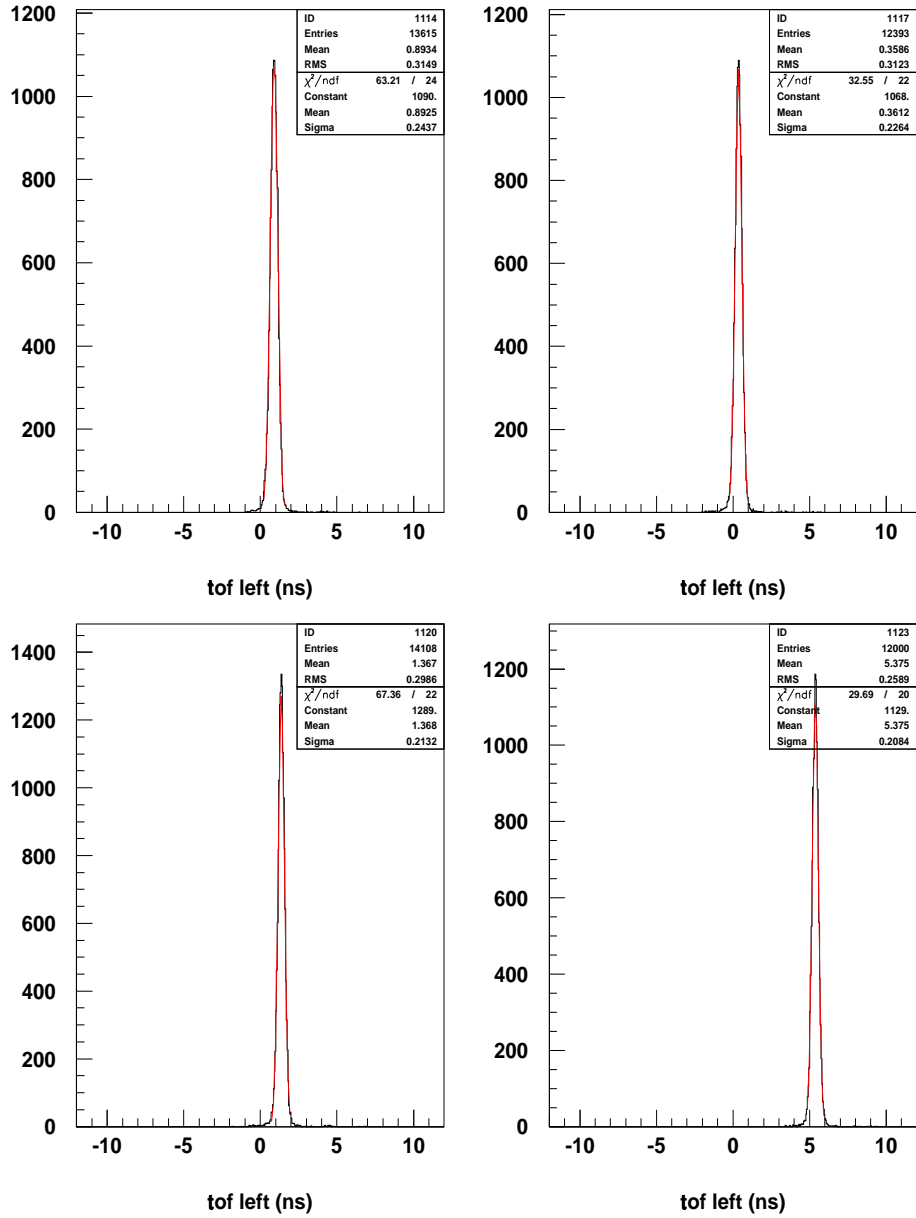


Figure 11:  $TOF_i$  distribution for  $i = 14, 17, 20$  and  $23$ , corrected for the time walk (left wall).



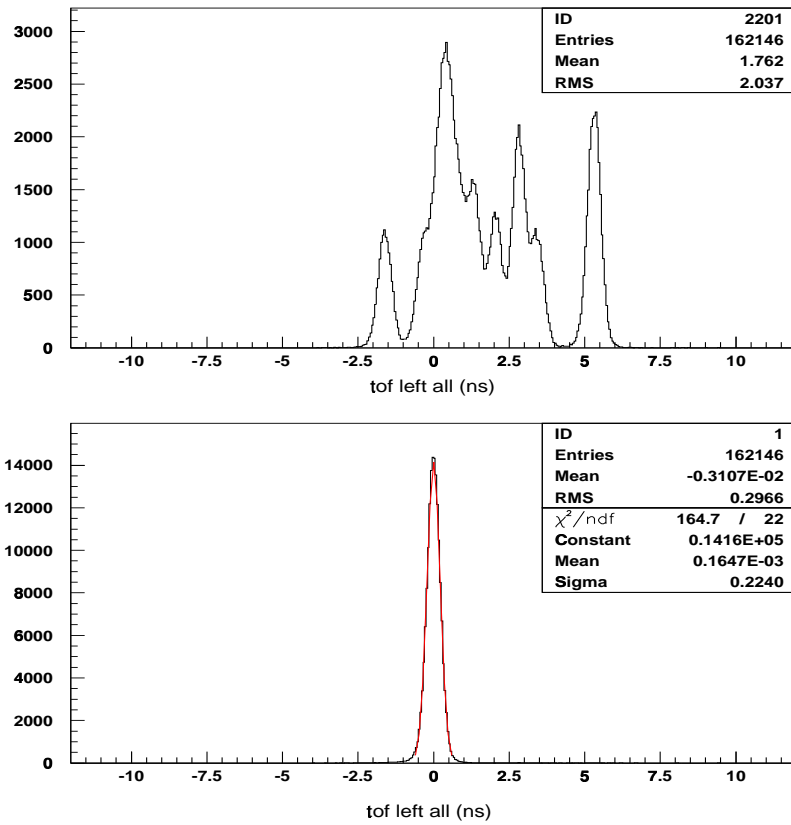


Figure 12: Overall distribution of the time-of-flight for the left wall, without (above) and with (below) the time corrections  $TOF_i$  described by eq. (5).

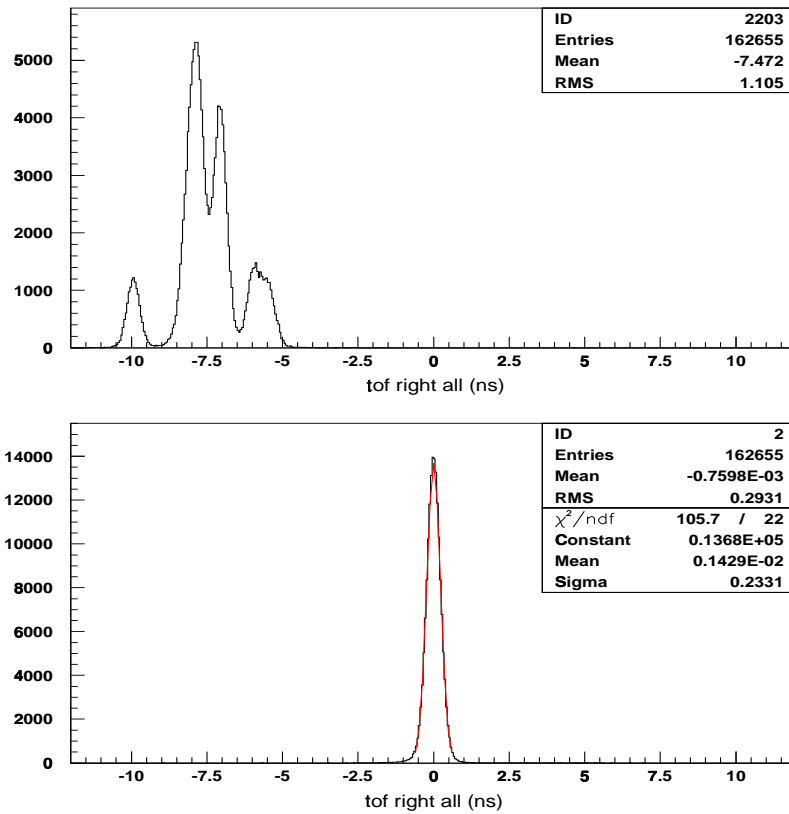


Figure 13: Overall distribution of the time-of-flight for the right wall, without (above) and with (below) the time corrections  $TOF_i$  described by eq. (5).

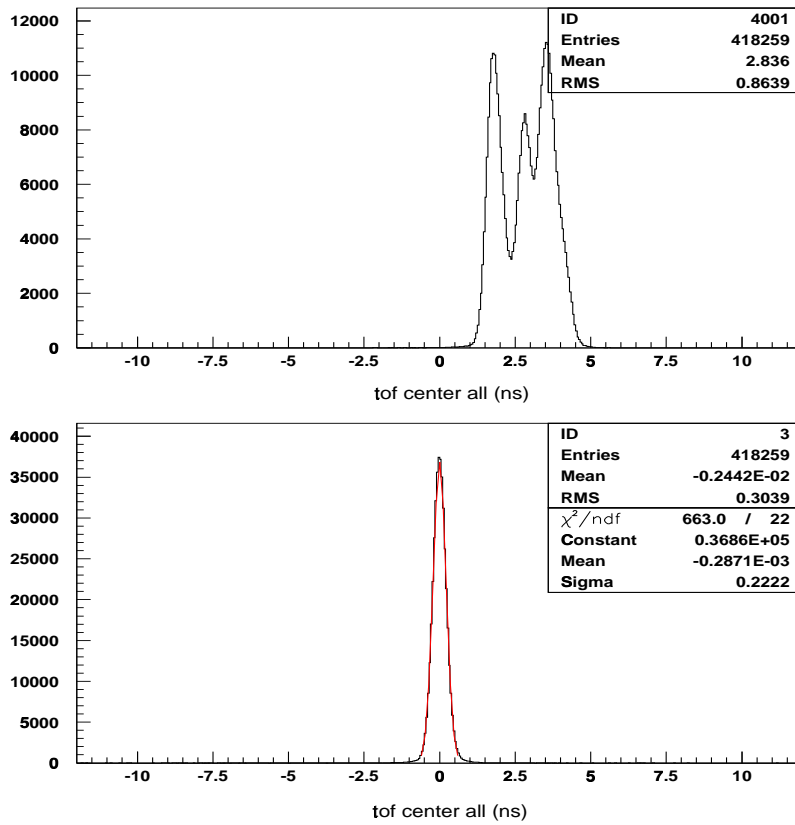


Figure 14: Overall distribution of the time-of-flight for the central wall, without (above) and with (below) the time corrections  $TOF_i$  described by eq. (5).

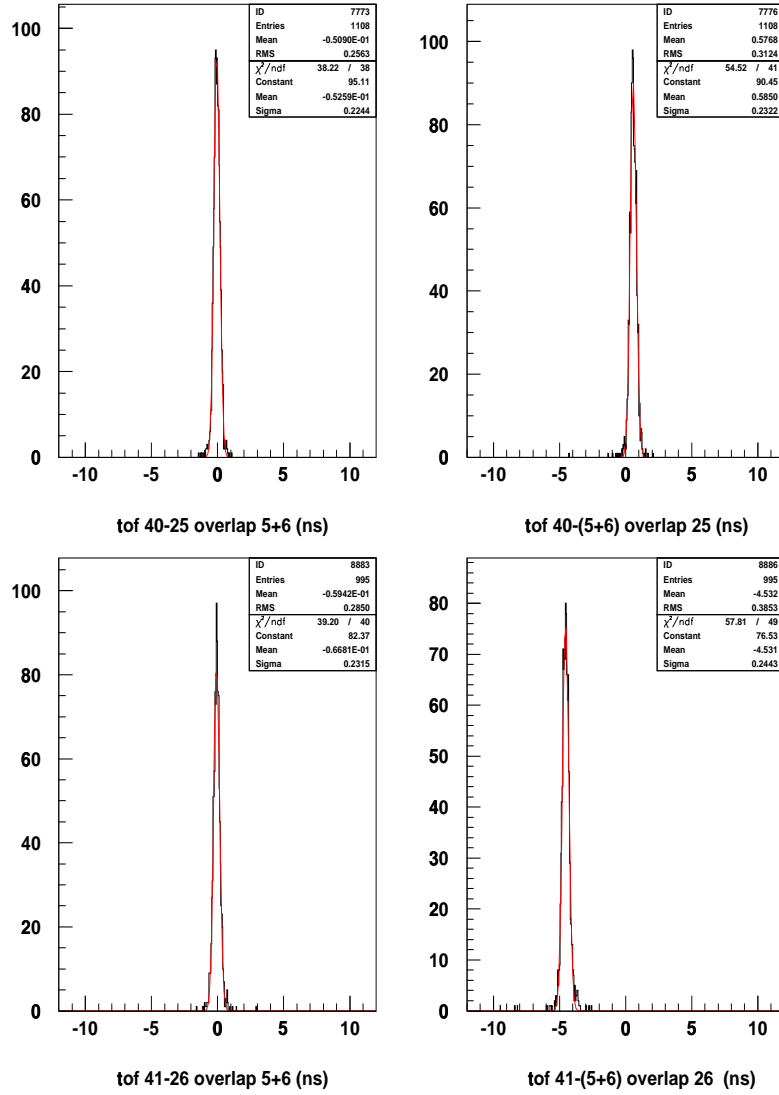


Figure 15: Distributions used in aligning the three walls. See the setup in Fig. 3 and the definition of times-of-flight in Sec. 3.3. Top figures refer to left-central walls:  $tof(40 - 25)$  (top left) and  $tof(40 - 5) + tof(40 - 6)$  (top right). Bottom figures refer to central-right walls:  $tof(41 - 26)$  (bottom left) and  $tof(41 - 5) + tof(41 - 6)$  (bottom right).

## 4 Conclusions

After their installation in the HARP experiment, the performance of the TOF-WALL scintillators has been monitored by collecting and studying cosmic events. Cosmic muons crossing the TOF-WALL counters at an angle  $\sim 50^\circ$  have been used to determine the time calibration constants of each counter with respect to a common time reference. The resolutions on the time-of-flight measurement turned out to be  $\simeq 225$  ps, after correcting for time-walk effects.

Assuming the same time resolution for the counters of the three walls and for the reference scintillators, the average intrinsic time resolution of the scintillators resulted to be  $\sigma_C \sim 160$  ps<sup>3</sup>, in agreement with laboratory tests [1].

In HARP, the time-of-flight of particles produced at the target is obtained from the difference between the times measured in the TOF-WALL and in the TOF B (or TDS) counter, which have an intrinsic time resolution of about 100 ps. Therefore the final time resolution on the t.o.f. is expected to be  $\simeq 190$  ps, considerably better than the design value of 300 ps.

## References

- [1] G. Barichello et al., "*The HARP TOF-WALL counter construction and test*", HARP Note 02-001.
- [2] M. Bonesini et al., "*Construction of a Fast Laser-Based Calibration System for the HARP ToF Counters wall*", submitted to IEEE 2002 Norfolk.

---

<sup>3</sup>This value should be corrected to take into account two geometrical effects that act in opposite directions: on one side the contribution due to the fluctuations on the flight distance ( $\sim 3$  cm) should be subtracted; on the other side the increase of signal for tracks at  $\sim 50^\circ$  improves the time resolution by about 20%. The two effects are roughly equal and cancel out.